Journal of Structural Geology 28 (2006) 494–507

JOURNAL OF STRUCTURAL GEOLOGY

www.elsevier.com/locate/jsg

Structural development of the Peregrina–Huizachal anticlinorium, Mexico

Y. Zhou *, M.A. Murphy, A. Hamade

Department of Geosciences, University of Houston, Houston, TX 77204, USA

Received 21 March 2005; received in revised form 5 November 2005; accepted 17 November 2005
Available online 25 January 2006

Abstract

The Sierra Madre Oriental fold belt is a NW–SE-trending contractional belt that spans nearly the entire length of Mexico. This area underwent Triassic–Middle Jurassic rifting and Late Cretaceous–Early Cenozoic shortening. Our structural investigation of the Peregrina–Huizachal anticlinorium in east central Mexico shows that its development is characterized by two phases of deformation: an early thin-skinned phase and a late thick-skinned phase. A detachment developed at the contact between the rift sedimentary rock and overlying limestone. During the thin-skinned phase, deformation of the Upper Jurassic–Cretaceous strata is accommodated by a series of detachment folds and faults. The rift boundary faults are sub-perpendicular to the late stage compression in east central Mexico. This makes rift-related faults prone to be inverted as reverse faults. During the thick-skinned phase, the basement in the rift is uplifted along two opposing reverse faults and experience internal deformation. Its uplift contributed to the growth of the Peregrina–Huizachal anticlinorium.

Keywords: Detachment; Anticlinorium; Basement reactivation; Red beds

1. Introduction

The Sierra Madre Oriental (SMO) fold–thrust belt stretches nearly 1500 km from northern to southern Mexico. It is an impressive expression of salt-influenced contractional deformation, map-view curve geometries, and widely considered to be thin-skinned and restricted to upper crustal levels (Padilla y Sanchez, 1985; Suter, 1987; Marrett and Aranda, 1999; Eguiluz de Antuñano et al., 2000). However, local exposures of Precambrian through Triassic rocks in the fold–thrust belt imply at least local involvement of basement during the development of the SMO fold–thrust belt (De Cserna, 1989; Perez-Cruz, 1993; Eguiluz de Antuñano et al., 2000) (Fig. 1). This apparent change in deformation style suggests that construction of the SMO fold–thrust belt was accomplished by structurally diverse mechanisms that may depend in part on the pre-existing tectonostratigraphic architecture of Mexico and on the types of rocks involved.

Exposures of Precambrian basement rocks occur in the Peregrina–Huizachal anticlinorium and Molango area (López-Ramos, 1985). These basement exposures are located within the frontal (eastern) portions of the SMO fold–thrust belt. The geometry and timing of basement-involved structures are not clear. Some studies have interpreted the basement to be bounded by Laramide-style high-angle reverse faults, postdating a thin-skinned phase of thrusting (Perez-Cruz, 1993; Eguiluz de Antuñano et al., 2000). Other interpretations show the pre-Jurassic basement as shallowly dipping thrust sheets, contemporaneous with supracrustal thin-skinned thrusts (Eguiluz de Antuñano et al., 2000). These two contrasting interpretations of the geometry result in significantly different estimates of total horizontal shortening accommodated in the SMO fold–thrust belt, with higher values of horizontal shortening for shallowly dipping faults and lower values for steeply dipping faults. In order to better understand the relationship between supracrustal contractional deformation, recognized throughout the SMO fold–thrust belt, and basement-involved structures, we conducted geologic mapping and structural analysis of faults and fractures from the Peregrina–Huizachal anticlinorium, a basement-cored anticlinorium in east-central Mexico (Fig. 1).

2. Geology of the Peregrina–Huizachal anticlinorium

From the end of the Cenomanian to the Maastrichtian, the structural framework of northern Mexico changed dramatically from extension represented by the Mexican Borderland Rift in northern and northeastern Mexico (De Cserna, 1989; Moran-Zenteno, 1994; Lawton and McMillan, 1999; Dickinson

* Corresponding author. Tel.: +1 713 7433413.
E-mail address: yong.zhou@mail.uh.edu (Y. Zhou).

0191-8141/$ - see front matter
doi:10.1016/j.jsg.2005.11.005

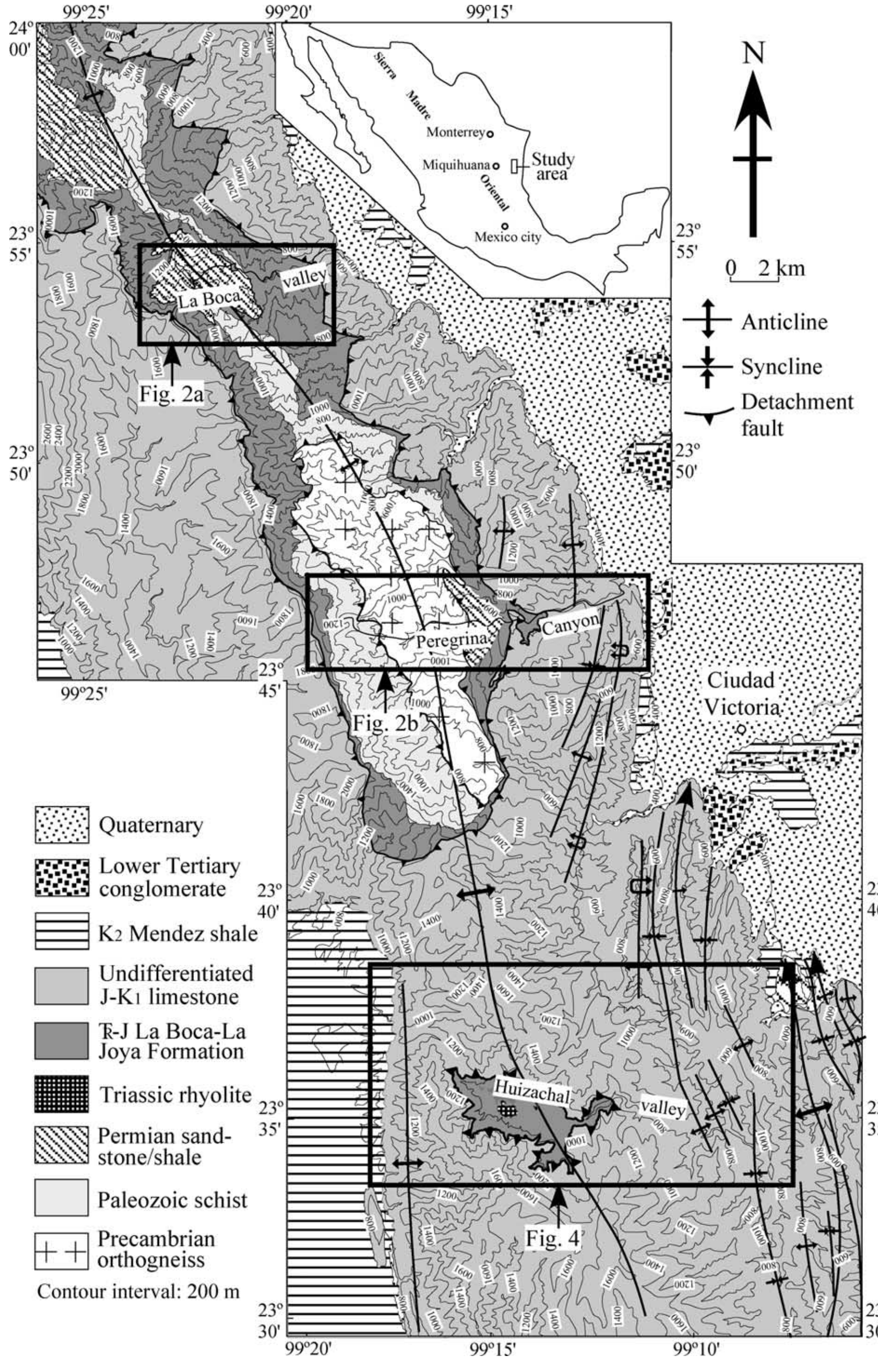

Fig. 1. Simplified geological map near Ciudad Victoria, Mexico (modified from INEGI (2000)).

and Lawton, 2001) to compression represented by the development of the SMO fold belt (Suter, 1987; De Cserna, 1989; Sedlock et al., 1993; Goldhammer, 1999; Marrett and Aranda, 1999; Eguiluz de Antuñano et al., 2000). In general, the fold belt detaches a thick sequence of Upper Jurassic through Cretaceous sedimentary rocks from Precambrian through Middle Jurassic metamorphic and sedimentary rocks (Padilla y Sanchez, 1982). Local exposures of basement occur near Ciudad Victoria (Carrillo-Bravo, 1961, 1965; López-Ramos, 1985).

The Peregrina–Huizachal anticlinorium (Fig. 1) is a north-northwest-trending, doubly plunging anticlinorium. We conducted geologic mapping at a scale of 1:50,000 along three E–W valleys that cut across the anticlinorium. From north to south, they are La Boca, Peregrina and Huizachal valleys (Fig. 1). The geologic framework of the anticlinorium may be viewed as consisting of two different components, each with a unique deformational history, a basement-complex and an overlying cover rock sequence.

2.1. Basement-complex

The basement-complex in the Peregrina–Huizachal anticlinorium consists of Precambrian metamorphic rocks, Paleozoic schist/sedimentary rocks, and Upper Triassic–Lower Jurassic red beds (Fig. 1). In La Boca valley, the Triassic–Jurassic red beds are underlain by Paleozoic schist and Permian sandstone/shale. In Peregrina valley, pre-Mesozoic rocks are composed of Precambrian gneiss, Paleozoic schist and Permian sandstone/shale (Garrison et al., 1980). The Precambrian gneiss is cut discordantly by granite dikes. Paleozoic biotite schist is in tectonic contact with Precambrian gneiss (Garrison et al., 1980). Permian sandstone/shale overlies onto the gneiss, and in turn they are overlain by Triassic–Jurassic red beds termed the Huizachal Group, which includes the La Boca Formation and overlying La Joya Formation (Mixon et al., 1959). The thickness of the Huizachal Group ranges from tens of meters to more than 2000 m (Mixon et al., 1959; Franco-Rubio, 1999). The La Boca Formation underlies either the La Joya Formation or Zuloaga Limestone of Late Jurassic age. In the type section in La Boca valley, the lower part of the La Boca Formation is composed of cobble-conglomerate. It rests on a topographically irregular surface. The basal strata are overlain by approximately 600 m of sandstones, siltstones and mudstones with many interbedded conglomerates. These are in turn overlain by approximately 325 m of sandstones and conglomerates (Mixon et al., 1959). La Joya Formation overlies La Boca Formation, Precambrian rocks or Paleozoic rocks and underlies Jurassic Zuloaga Formation; in some places the La Joya Formation is missing and the Zuloaga Formation rests on the La Boca Formation (Mixon et al., 1959). The La Joya Formation is composed of conglomerate, sandstones and mudstones. In the Huizachal Valley, felsic rocks intruded the La Boca Formation (Fig. 1), and this intrusion locally metamorphosed the La Boca sandstone (Belcher, 1979) into quartzite.

2.2. Cover rock sequence

Stratigraphically above the La Boca and La Joya Formations is an approximately 2-km-thick sequence of marine sedimentary rocks (Fig. 1). This sequence is dominated by Jurassic–Cretaceous limestone and shale. The carbonate strata are a laterally heterogeneous patchwork of basinal and platformal sequences (Wilson, 1990). A complete cover sequence is exposed along the flanks of the Peregrina–Huizachal anticlinorium. Based on previous studies in the Peregrina valley (Carrillo-Bravo, 1961, 1965), the Upper Jurassic limestone is composed of three formations, Zuloaga (∼50 m), Olvido (∼200 m) and La Casita (80 m) Formations. They are widely distributed throughout the Sierra Madre Oriental (López-Ramos, 1985). The Zuloaga Formation is interpreted to represent a transgressive sequence with shallow-water limestones (Barboza-Gudino et al., 1999). The Olvido Formation of Kimmeridgian age consists of a lower portion of shales and an upper portion of predominantly carbonate rocks (Padilla y Sanchez, 1982; Salvador, 1987; Goldhammer, 1999). This formation is overlain by the La Casita Formation. The lower part of La Casita Formation is limestone, and the upper part is shale. Stratigraphically above, Cretaceous strata consist of a thick sequence of limestone and shale. The limestone (∼800 m) can be divided into five formations, Taraises, Tamaulipas, Cuesta del Cura, Agua Nueva and San Felipe Formations from bottom to top. The San Felipe Formation is overlain by Upper Cretaceous Mendez shale (∼800 m). It is widely distributed in SMO, but in many areas this shale has been eroded, particularly along the crests of large anticlines.

3. Structural analysis

The Peregrina–Huizachal anticlinorium trends NNW–SSE and can be traced for at least 200 km. To the south, the anticlinorium dies out at ∼23°10′N. Below, we present the outcomes of our structural analyses of structures exposed within the Peregrina–Huizachal anticlinorium. Structural data were collected at regularly spaced intervals across the Peregrina–Huizachal anticlinorium along traverses in the La Boca, Peregrina and Huizachal valleys. Locations where structural measurements were taken are indicated on our geologic maps as L#, P#, and H#, corresponding to locations in La Boca, Peregrina, and Huizachal valleys, respectively. Based on crosscutting relationships, we categorize structures into one of three stages: pre-SMO deformation, thin-skinned deformation and basement-involved deformation.

3.1. Pre-SMO deformation

Structures within the La Boca and Peregrina valleys are very similar. Our mapping shows that the Peregrina–Huizachal anticlinorium is cored by Precambrian gneiss, Paleozoic schist, Permian sandstone/shale and Triassic–Jurassic red beds (Fig. 2a and b). Structures in these rocks change in structural style and deformation regime. Ductile shear zones in Precambrian gneisses were observed in outcrops and in thin-sections. Their attitude varies across the hinge line of the anticlinorium. On the western flank, shear zones and foliations strike nearly E–W, dipping mainly to the north (Figs. 2b and 3a). Across the hinge line, shear planes and foliations on the eastern flank principally strike ∼N–S to NE–SW, dipping to the E–SE (Figs. 2b and 3b).

Foliations in Paleozoic schist generally strike NW–SE to NE–SW. Fault planes within the Paleozoic schist strike northeast and dip steeply to the northwest. They contain mineral stretching lineations and shear fabrics that indicate reverse right-slip motion (Fig. 3c). These schists are intruded by pegmatite. Both schists and the pegmatite are cut by late stage shear zones that strike northwest and dip steeply (82–70°) towards the northeast. These late stage shear zones contain mineral stretching lineations that have low rakes indicating dominantly left-slip motion (Fig. 3d).

Away from the shear zone, both Precambrian gneiss and Late Paleozoic pegmatite intruding biotite schist have a distinctive feature with development of subgrains within plagioclase, quartz, and garnet. These subgrains form a mosaic

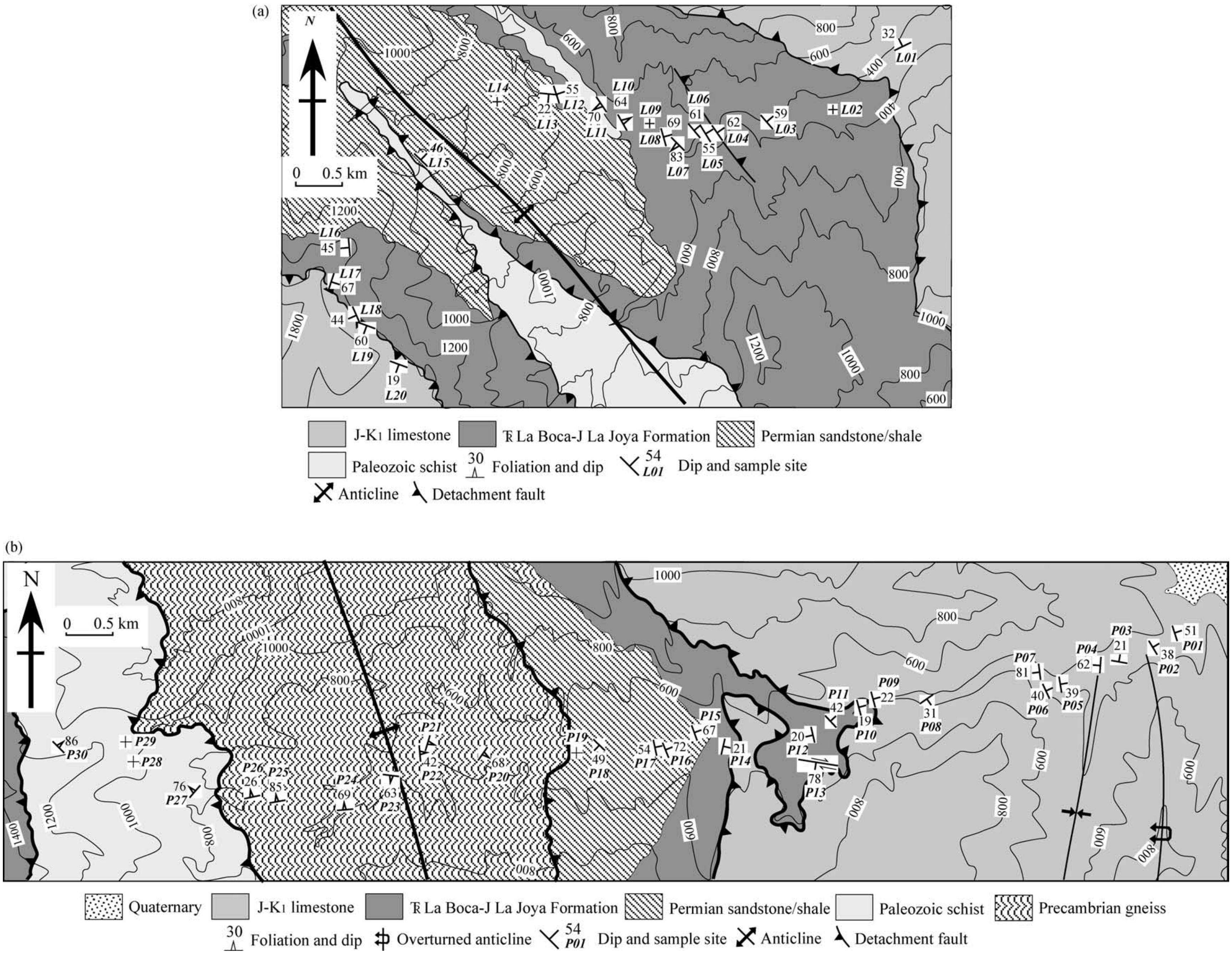

Fig. 2. Geological map along La Boca valley (a) (after our mapping and INEGI (1970, 1977)) and Peregrina Canyon (b) (after our mapping and INEGI (1978)).

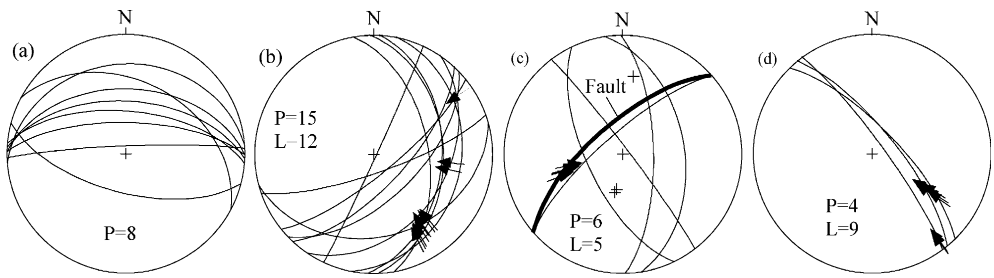

Fig. 3. Plots of lower hemisphere equal-area stereonet of structural data from Peregrina valley. (a) Shear planes in Peregrina orthogneiss from sites P23–P26; (b) shear planes and striations (arrows indicating the hanging wall movement direction, hereafter the same) in Peregrina orthogneiss from sites P20–P22; (c) faults (thick lines), foliations (thin lines), lineations (arrow) and fold axes (crosses) from Peregrina schist from sites P27–P30; (d) shear planes and lineations from Peregrina pegmatite at P28.

texture, commonly observed in thin sections from Triassic–Jurassic sandstone and conglomerate, suggesting that the gneiss and pegmatite experienced a penetrative brittle deformation prior to the deposition of overlying red beds. Even though the Permian and Triassic–Jurassic sedimentary rocks underwent strong deformations in the La Boca–Peregrina structural window, gneiss and other metamorphic/igneous hard rocks are not affected by the late deformation. This is indicated by the different structural trend/style and deformation regime between the hard basement and overlying rocks.

3.2. Thin-skinned deformation

3.2.1. La Boca valley

At the western end of the La Boca transect, Upper Jurassic limestones lie sub-parallel to the underlying La Joya Formation. The limestones vary between 1 and 3 m thick and dip at low–intermediate angles toward the southwest. Deformation of these rocks is dominated by bedding-parallel shear. Bedding-parallel shear is expressed by high-strain, low temperature deformation. Locally, approximately 30-cm-thick cataclasite is present in the hanging wall and approximately 5-cm-thick cataclasite is present in the footwall. At distances exceeding approximately 30 cm structurally upwards from sliding surfaces, no trace of cataclasis is observed. Away from the sliding surface, cataclastic grains increase in size and cataclastic cleavage planes, composed of relatively flat surfaces of cataclasts aligned subparallel to each other, increase in spacing. They are generally parallel to the bedding. Although strongly sheared, no significant displacement occurred between grains. Sometimes, stylolite is preserved with teeth normal to bedding. Since bedding-parallel faults do not display bedding normal shortening as indicated by stylolites, the bedding-parallel slip was posterior to the failure of stylolite teeth. Slip directions on bedding-parallel faults are top-to-east based on en échelon vein array of tension gashes.

3.2.2. Huizachal valley

No pre-Mesozoic rock is exposed along this transect (Fig. 4). The first-order structure exposed in the valley is the large Peregrina–Huizachal anticlinorium and a detachment (Figs. 4 and 5a) separating the cover rock sequence from the underlying Triassic–Jurassic red beds. The flanks of the anticlinorium are asymmetrical (Fig. 5a). Second-order folds in the cover rock sequence are defined by several box folds with wavelengths varying from hundreds of meters to a few kilometers. Third-order folds in the cover rock sequence are represented by a series of meter-scale asymmetrical folds with wavelengths <10 m.

3.2.2.1. Structures east of the structural window. The easternmost second-order fold has a wavelength of approximately 3.3 km. Our mapping shows that this fold is approximately symmetrical in the upper part. The hinge zone is cylindrical; the western flank shallows westward, and ultimately bends sharply with a box shape. At the core of the fold, a thrust fault merges with an east-directed bedding-parallel fault. Shear fractures define a 1–2-m-thick shear zone.

Along the highway, structures in the eastern flank and core of the above-mentioned box fold are classified into third-order structures. They are a series of chevron, box, and rounded folds. The wavelength of the folds decreases from east to west. Thinly bedded limestones in the eastern half of the profile are folded into broad synclines and anticlines. In contrast, structures in the western half of the profile are strongly affected by the large eastward vergent thrust. They are characterized by short-wavelength box and chevron folds. These folds are symmetrical to asymmetrical. Locally, they are cut by reverse faults with minor offsets. A well-developed box fold is exposed along the highway road cut. The outer arcs are box shaped and can be described as a symmetric conjugate kink fold. In the inner arcs of the fold, the axial planes merge. The space problem is resolved by a cuspate anticline, kink wedge fold (Johnson, 1977).

At H06, the aforementioned large thrust juxtaposes a hanging wall flat over a footwall ramp. The fault dips 27° towards 212°. The fault zone is marked by a penetrative cleavage. Cleavage and thin limestone beds curve asymptotically towards the fault plane. The cleavage–fault relationship, together with the orientation of tension gashes in the hanging wall, indicates top-to-east motion. On the fault plane, isolated limestone blocks could be seen with long axes parallel to the fault. Competency contrast is obvious between the thick-bedded limestone and the argillaceous thin limestone in the hanging wall. This contrast produced the boudinage of the competent layer by stretching and necking due to shearing

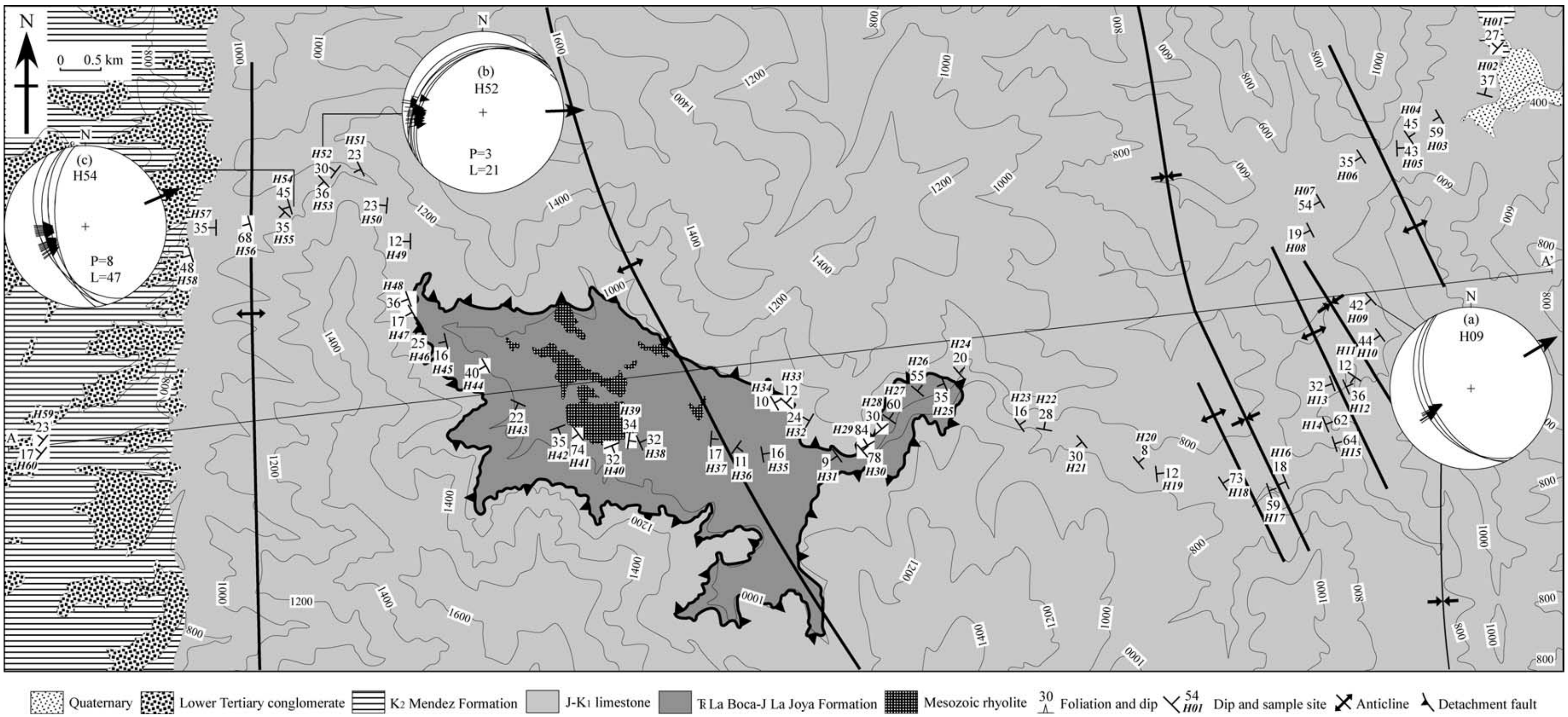

Fig. 4. Geological map along Huizachal valley (after our mapping and INEGI (1978)). Inserts indicating lineation on fault planes. (a) Site H09; (b) site H52; (c) site H54.

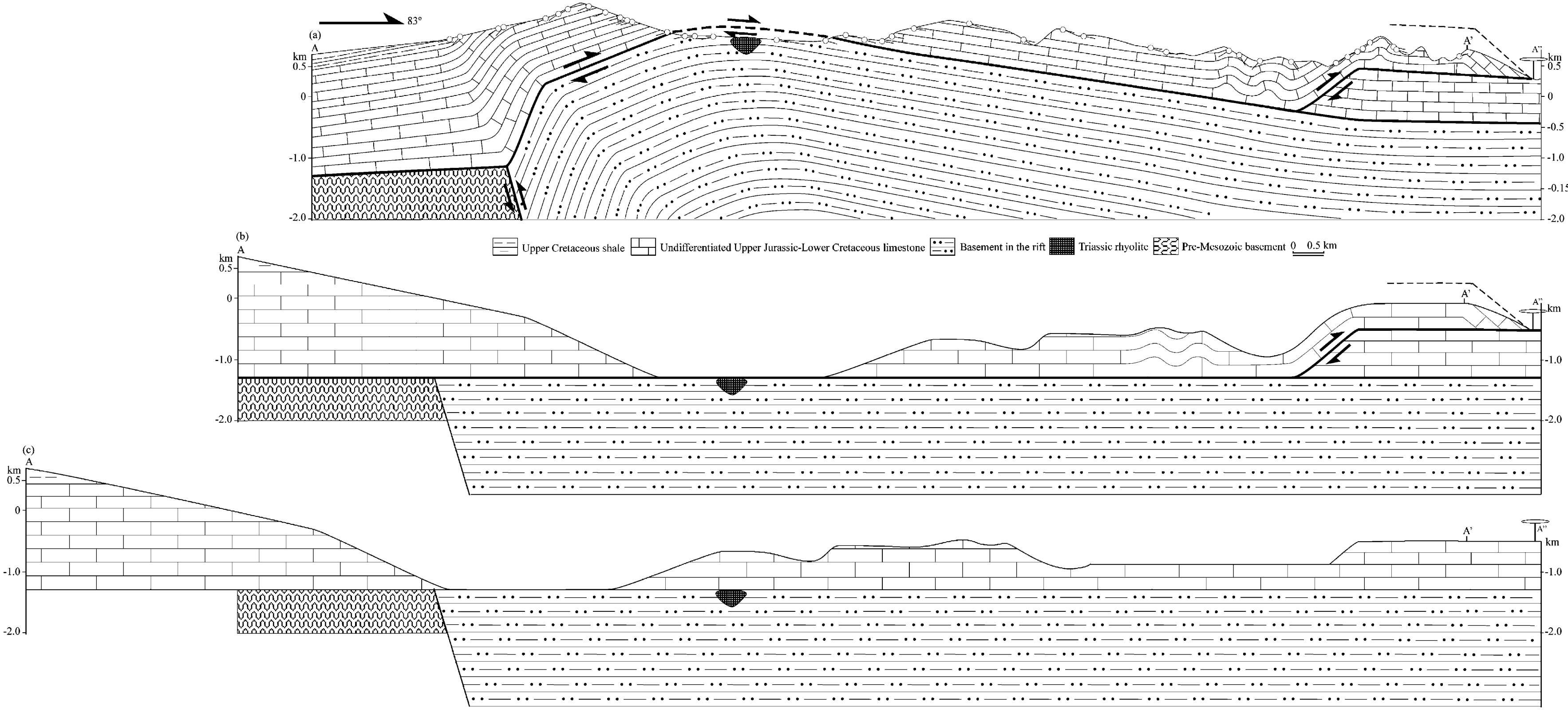

Fig. 5. (a) Cross-section along Huizachal valley. Segment A′A″ is projected to the east; (b) the easternmost second-order anticline and folding due to the basement uplift are removed; (c) displacement along the fault and folding in the cover sequence are removed.

along the fault surface. The footwall is intensely brecciated. A cataclastic zone is approximately 2 m thick, indicating that the footwall underwent a strong deformation. The fragmented clasts are angular and cemented. Their long axes are roughly parallel to each other near the fault plane, but away from the fault they are randomly distributed, and the clasts increase in size. This suggests that intensity of deformation is greatest near the fault. Early stage fractures in the fragments are usually filled with calcite. They terminate at the clast boundary. Both the fragments and matrix are cut by late stage conjugate fractures without filling. The acute angle of the conjugate fractures faces towards SW–NE, implying that they formed during slip on the overlying thrust.

Strength of bedding contact is relatively weak within layers, as demonstrated by flexural slip along bedding surface. Spectacular slickensides and slickenlines developed along the bedding planes within intermediate–thick limestones. These sliding planes commonly dip 42–51° to ~236° at site H09. Lineations, including grooves and calcite fibers, are present on the slickensides. They are aligned in an approximately down-dip direction. Slip directions are tightly grouped around a mean of 58° at H09 (insert (a) in Fig. 4). Step structures indicate a clear reverse sense of motion. The spectacular slickensides and slickenlines indicate that sliding along the bedding surface is an important mechanism to accommodate deformation.

Another two large second-order anticlines are well-exposed approximately 200 m to the north of the highway at H13 (Fig. 6a) and H17, respectively. The fold at H13 verges towards the east and is cored by a series of disharmonic folds, including chevron and rounded folds (Fig. 6b), depending on the bedding thickness and position within the fold. In thin limestones, chevron folds developed in the inner arc of the fold; in the outer arc, they have a rounded hinge. With increase in bed thickness, the folds have rounded hinges in both inner and outer arcs (Fig. 6c).

From site H19 westward to the contact between the Triassic–Jurassic red beds and Jurassic limestone, deformation is relatively weak. Limestones as a whole dip gently to the E–NE (Figs. 4 and 5a).

3.2.2.2. Structures in the structural window. A detachment at the contact between the Zuloaga Formation and the La Joya Formation can be traced along the entire margin of the structural window (Figs. 1 and 4). This detachment is broadly folded about the axis of the Peregrina–Huizachal anticlinorium. In general, the detachment juxtaposes similar rock units along the margin of the structural window. On the western and eastern margins, the fault juxtaposes red mudstone/sandstone (La Joya Formation) in its lower plate against overriding interbedded limestone and shale (Zuloaga Formation). In the central part of the structural window, the detachment emplaces thickly bedded limestone against sandstone. No thin limestone/

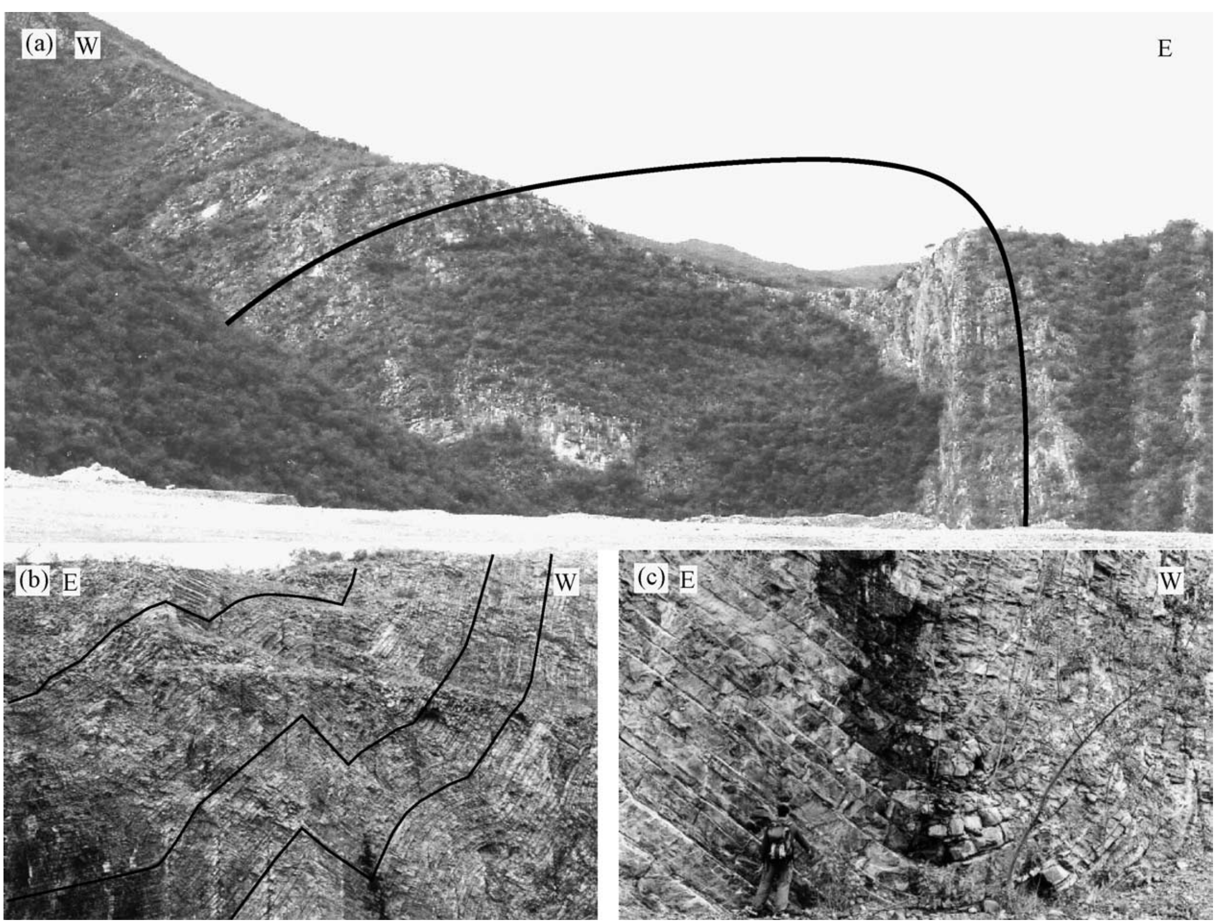

Fig. 6. (a) Second-order anticline outcropped near site H13, (b) and (c) chevron and rounded folds in the core of the fold.

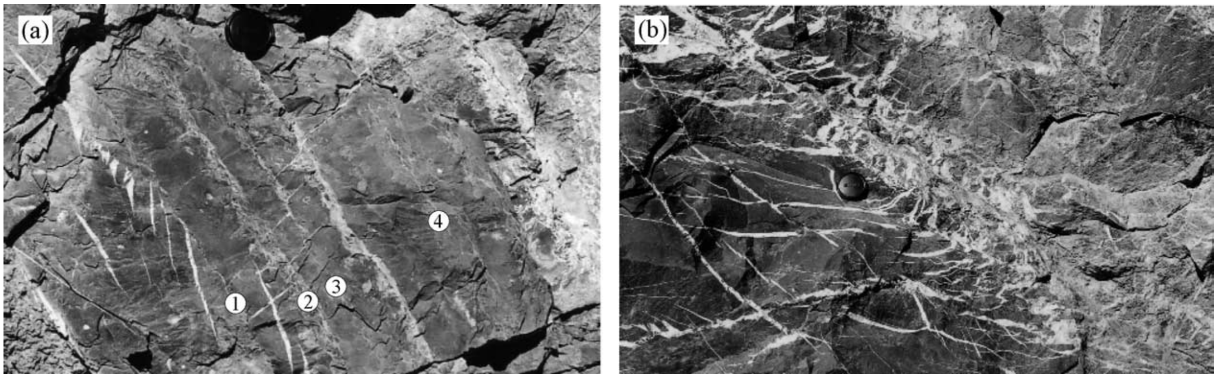

Fig. 7. (a) Layer-parallel cataclasites 2–4 cm thick, (b) faults initiate and grow from continued development of echelon tensional gashes. Site H30.

shale transitional zone exists. This transition zone is also missing in the La Boca and Peregrina valleys, where the detachment places thickly bedded limestones onto conglomerate. The missing transitional zone may be explained by the presence of a paleotopographic high in the central part of the Peregrina–Huizachal anticlinorium. In this scenario, interbedded limestone and shale were deposited at local topographic lows. This is in line with a sedimentary wedge composed of interbedded limestone and shale on the eastern margin of Huizachal window. The cover rocks near the structural window dips gently (5–20°) to the east or to the west (Fig. 5a).

Limestones contain layer-parallel cataclasites, 2–4 cm thick. They usually serve as weak zones for fault development. Faults also initiated and grew from continued development of échelon tensional fractures and sigmoidal tension gashes (Fig. 7a and b), indicating that these tensional structures played some role in accommodating strain during deformation.

On the western margin of the structural window (sites H43–H48) (Fig. 4), the La Joya red beds grade upward into Zuloaga limestone/argillite. This graded sequence is dominated by 10–30-cm-thick sandstone beds at the base, thick argillite in the middle that is interbedded with 10–20-cm-thick limestone beds at the top. No discrete detachment surface is observed in this sequence. Rather, numerous bedding parallel slip surfaces and small reverse faults in the thin sandstone embedded in the argillite are common throughout. We interpret that eastward translation of the cover rock sequence was mainly accommodated by flexural slip in the limestone and flexural flow in the argillite.

3.2.2.3. Structures west of the structural window. Outcrops from H49–H51 are within the lower part of cover rock sequence. The cover rock sequence is characterized by thinly bedded limestones, and is weakly deformed. Strata generally dip to the west with a low angle (10–25°) (Figs. 4 and 5a). To the west, dip data show that the cover rock sequence is folded into a west-vergent anticline. This anticline can be traced for several kilometers (Figs. 1 and 4). Its hinge zone lies at site H56. It extends approximately 2 km to the north and approximately 10 km to the south. The cover rock sequence to the east of the fold hinge dips 30–45° to the southwest between H52 and H55 (Figs. 4 and 5a). By contrast, the western limb dips steeply to the west (68°) (Figs. 4 and 5a).

Slickensides developed due to bedding-parallel flexural slip. They are coated with a thin layer of striated red gouge/calcite; lineations on bedding-parallel faults plunge to the west. Their rakes range from 30 to 45° with a mean trend of 269° (insert (b) in Fig. 4), indicating a slip direction of 89°.

Internal deformation of the cover rock sequence increases from east to west. At sites H54 and H55, two east-directed thrust faults are observed with attitudes of 239°/35° and 211°/62°, respectively. These faults converge at depth. The displacement for the lower fault is approximately 1 m. Upward, this fault branches into two faults, and the displacement is progressively transferred into the overlying beds at the tip. Grooves and calcite fibers on southwest dipping fault surfaces have high rakes ranging from 70 to 80°, and display a mean trend of 253°, indicating a transport direction toward 73° (insert (c) in Fig. 4).

Other meso-scale structures are also present. They shed light on the deformation history. A small east-dipping backthrust occurs along bedding and cuts the fold backlimb. West-dipping thrusts directly below the backthrust resulted in development of fault-bounded horses. The horse stack pattern indicates an eastward movement. Faults cutting the anticline core have opposite senses of displacement, suggesting that both limbs of the anticline moved toward the hinge and that the bedding surfaces were active during flexural slip.

3.3. Basement-involved deformation

Basement-involved deformation displays two first-order aspects: uplift and internal deformation. Relative uplift of the basement varies from north to south (Fig. 1). The highest projected Mesozoic red beds lie at approximately 1900 m above sea level in La Boca valley, at approximately 2300 m in Peregrina Canyon and at approximately 1150 m in Huizachal valley. Our mapping shows that the average vertical differential displacements from their regional stratigraphic position are at least 3500 m in La Boca valley, 3900 m in Peregrina Canyon and 2750 m in Huizachal valley assuming a constant thickness of the cover sequence (~2000 m) in which the top lies at 400 m in the foreland plain.

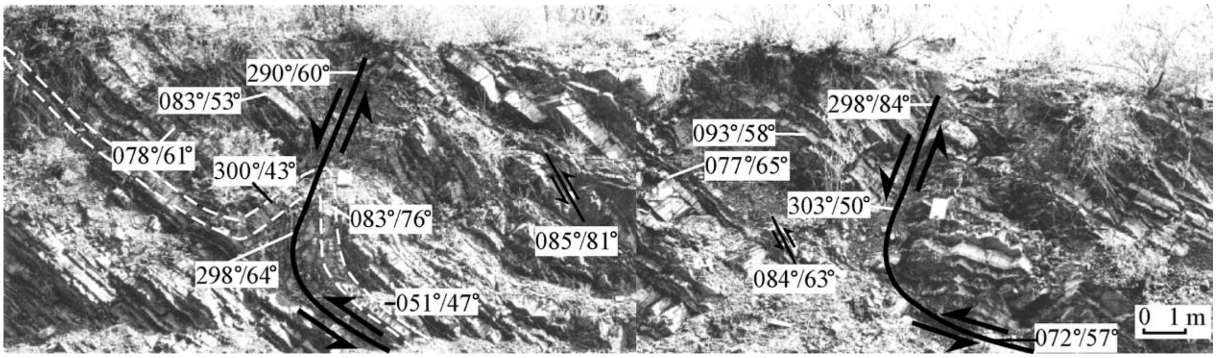

Fig. 8. Structures in Permian sandstones/shales at P17 from Peregrina Canyon.

Internal deformation is prevalent throughout the Permian and Mesozoic sedimentary rocks in the La Boca–Peregrina structural window. Compared with the overlying limestone, most of these basement rocks are weak due to the presence of mudstone/shale and minor gypsum. These lithologies are prone to be involved in deformation. Permian sandstone and shale overlie Paleozoic schist in the La Boca valley (Fig. 2a). Wedge faults are common throughout the Permian thin sandstone. These faults are inclined (~20°) to bedding. Other structures within the upper part of the Permian sandstone/shale are well developed. At site P17 (Fig. 2b), fault surfaces (050–075°/47–57°) develop along bedding planes, step upward (290–303°/50–84°), cut across overlying layers at a high angle, and ultimately die out (Fig. 8). Based on the asymmetry of folds and offset of marker horizons, the shear sense of these faults is from east to west. Vergence of the fault/fold, fault-slip data and brittle deformation regime are in accordance with those in the overlying Triassic–Jurassic red beds in the La Boca and Peregrina valleys. Therefore, we interpret these structures to have formed during the development of the SMO fold–thrust belt.

Reverse faults are common in the Triassic–Jurassic red beds. One fault dips 49° to 070° at L04. Slickensides dip steeply NEE and SWW. Grooves and striations on the slickensides have rakes ranging from 20 to 55° (Fig. 9a). The hanging wall is deformed into a west-verging overturned anticline. Chatter marks and geometric relationship between shear cleavage and fault surface, combined with the fold asymmetry, indicate reverse movement towards the west with some horizontal component. The shear sense is in agreement with en échelon tension gashes (324°/42°) (Fig. 10a). Locally, conglomerate layers are cut by steeply dipping faults. The strata in between are sheared into a ‘type I’ S–C fabric (Lister and Snoke, 1984). The C surfaces dip to 226° at 78°. This S–C fabric indicates that the east side is up (Fig. 10b).

Another set of faults developed in the La Boca–Peregrina structural window. These faults strike NW–SE, and dip steeply to the northeast or southwest. Calcite fibers and grooves plunge at a low angle (10–20°) (Figs. 9b and 11a), indicating a dominant horizontal slip component. A left-lateral shear sense is determined from step structures. The shear sense agrees with that indicated by fold asymmetry with a steep axial plane (Fig. 11b). Their formation could be explained by eastward protrusion of the southern area. These faults most probably functioned as transfer zones to accommodate increasing eastward movement to the south.

Basement structures in the Huizachal structural window are east-vergent. Immediately below the detachment along the eastern margin (H25–H27), mudstone is intercalated with gypsum. These weak layers have been deformed into east-vergent asymmetrical and overturned folds. Gypsum layers are locally thicker in the cores of folds. Other structures in the Mesozoic red beds include drag fold and subvertical slickensides. Thin sandy mudstone of the La Joya Formation lies beneath the detachment. It is deformed into asymmetrical folds (Fig. 12). Axial planes dip to the west, indicating eastward movement. The folded layer is at least 4 m thick, and its flanks do not show obvious changes in attitude and length. This indicates that the deformation related to slip along the detachment is not limited to the sliding plane. Fractures are widely developed in the La Boca–La Joya sandstones. They usually dip steeply and have low-rake slickenlines.

4. Structural model and discussion

4.1. Structural model

Two results have chiefly motivated construction of the structural model described below (Fig. 13); (1) the cover rock sequence is detached from the underlying basement complex, and (2) this detachment is folded and associated with local uplift of the basement complex.

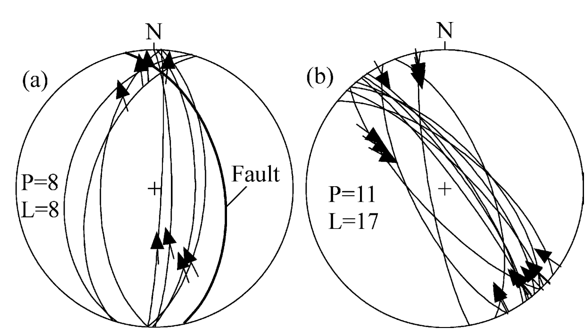

Fig. 9. Plots of lower hemisphere equal-area stereonet of structural data from La Boca valley. (a) Lineations on slickensides at L04; (b) lineations on slickensides from red beds in La Boca valley.

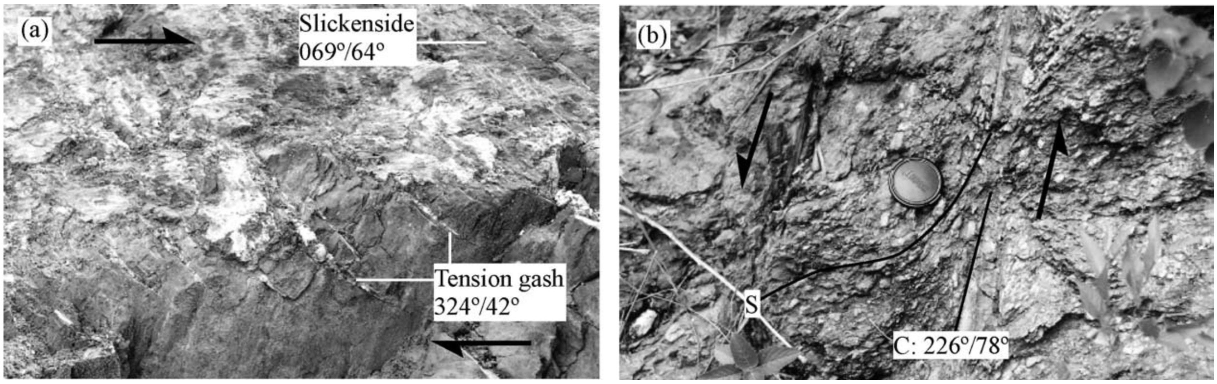

Fig. 10. (a) Tension gashes and slickensides at L10, (b) shear cleavages in conglomerate at L07.

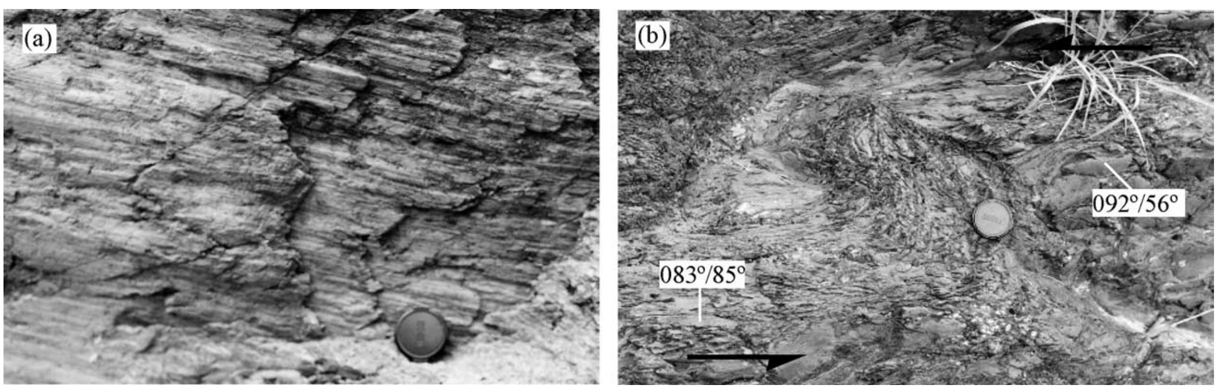

Fig. 11. (a) Calcite fibers on steep slickensides on bottom side at L04, (b) asymmetrical fold at L05.

Rifting during the Late Triassic and Jurassic resulted in deposition of the La Boca and La Joya Formations (Fig. 13a). These rock units are locally exposed throughout east-central Mexico (Mixon et al., 1959; Carrillo-Bravo, 1961; López-Ramos, 1985; Salvador, 1987; Franco-Rubio, 1999). The red beds represent alluvial fan, fluvial, and lacustrine depositional settings and are interpreted to be deposited in graben systems (Salvador, 1987; Goldhammer, 1999). These basins are interpreted to form a semi-continuous north-northwest-trending chain (López-Ramos, 1985; Salvador, 1987; Goldhammer, 1999). The depositional environment changed from a continental fluvial to a shallow marine environment in the Oxfordian (159–154 Ma) (Bacon, 1978), resulting in the accumulation of an approximately 2-km-thick sequence of carbonate platform rocks (Fig. 13b). The SMO fold-belt initiated sometime after deposition of the Mendez shale (84–66.4 Ma) (López-Ramos, 1985).

Fig. 13c shows initiation of the SMO fold–thrust belt as a thin-skinned fold–thrust system. A detachment fault develops at the contact beween the Zuloaga Formation and the La Joya

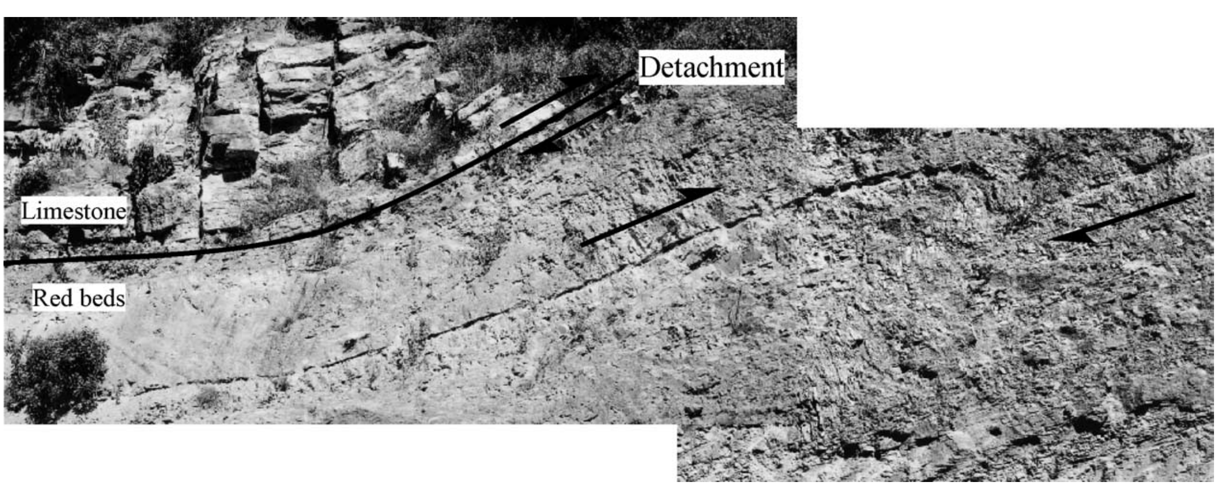

Fig. 12. Regional detachment with an asymmetrical fold vergent to the east at site H31.

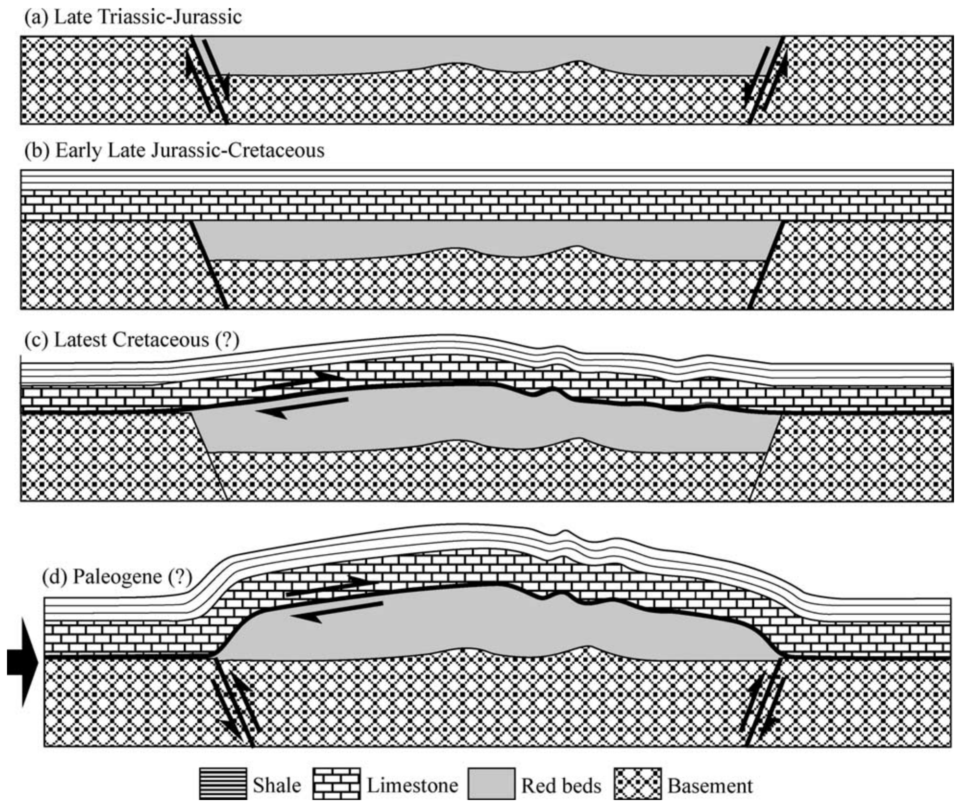

Fig. 13. Structural model of the Peregrina–Huizachal anticlinorium. (a) Development of rift basin and deposition of red beds in Triassic–Jurassic time, (b) deposition of Upper Jurassic–Lower Cretaceous limestone and Upper Cretaceous shale, (c) the cover rocks detached along the basement–cover rock contact and folded during Late Cretaceous (?), (d) continued compression resulted in the reactivation of rift basin faults and rise of the basement during Paleogene (?).

Formation. The structural windows indicate that the detachment horizon in this area is the Triassic–Jurassic red beds. One explanation for the position of the detachment is the contrasting competence and deformation between the cover rocks and the basement. The cover rocks are mainly composed of intermediate–thick competent limestone, and have abundant large to small box folds and faults, suggesting that they have undergone strong deformation. However, the basement rocks, composed of incompetent red beds (mudstone, sandstone, conglomerate, and minor gypsum), are relatively weakly deformed in the Huizachal structural window. This marked contrast in competency and obvious difference in deformation intensity imply that the contact between the limestone and the red beds should be the principal detachment surface. This is supported by drag fold just below the Jurassic limestone and concentrated shear cleavage in the Upper La Joya mudstone. The position of the detachment surface is also confirmed by other structural windows and by borehole data (Basanez-Loyola et al., 1993; Wilson and Ward, 1993). Thus, for those flat areas in the SMO, the detachment depth is approximately 2000 m corresponding to the thickness of the cover sequence; for those strongly deformed areas, the hanging wall should be thicker ($\sim$3000 m) due to folding and thrust stacking. Our fault-slip and structural trend data indicate that movement along the detachment is east-directed.

Fig. 13d shows the late stage development of the Peregrina–Huizachal anticlinorium. Our model explains that slip along steeply dipping reverse faults results in uplift of the basement complex as well as folding of the overlying detachment. Basement uplift is documented by exposure of Precambrian–Jurassic rocks $>$2700 m above their projected regional elevation. The eastward and westward vergent structures in the rift sedimentary rocks are ascribed to the disturbance of the hard basement as described below. A line–length balanced cross-section along the Huizachal transect yields approximately 19% ($\sim$4.62 km) shortening for the cover rocks during the thin-skinned and thick-skinned phases (Fig. 5b and c).

4.2. Discussion

There is a strong correlation between high topography and basement complex exposures at the two structural windows. Cross-section construction suggests that Mesozoic sedimentary rocks have been uplifted 2700–3900 m and that the detachment fault lies above its regional elevation in the structural windows. We suspect that pre-existing normal faults in the basement may have been reactivated as high angle reverse faults to facilitate uplift of the basement complex. This is because normal faults are zones of low frictional resistance in the crust due to alteration, cataclasis, water weakening and high pore-fluid pressure along the fault compared with shear rupture strength of unfractured rock (Etheridge, 1986; Sibson, 1993; Holdsworth et al., 1997; Marshak et al., 2000). These faults can be reactivated under low lateral differential stress (Cooper and Williams, 1989). Moreover, rift-related normal faults have widely been interpreted to strike north-northwest in this area

(López-Ramos, 1985; Salvador, 1987; Goldhammer, 1999), which would be optimally oriented to be reactivated during E–W shortening.

Structural analyses show that rift normal faults are inverted and truncate the cover sequence in the Rocky Mountains (Marshak et al., 2000), Zagros fold belt (Jackson et al., 1981; Sherkati et al., 2005), Apennine thrust belt (Butler et al., 2004) and northwest Argentina (Kley et al., 2005). Compared with these thick-skinned deformation areas, there are two prominent structural differences in the study area. (1) No emergent thrust had been observed to cut across the cover rocks above the projected rift boundary faults; and (2) deformation of Permian and Mesozoic sedimentary rocks is strongly influenced by Proterozoic and Paleozoic competent igneous and metamorphic rocks.

An important reason for lack of the emergent thrust could be explained by incompetence of the red beds in the rift basin. Even if the pre-existing normal faults are reactivated as reverse faults, the red beds can migrate toward the anticline core where less stress is present. Due to this lateral movement, the force exerted by the red beds just above the rift faults is not strong enough to break the overlying competent limestone. This may explain why no thrust extends from the basement into the limestone.

Paleozoic and older metamorphic and igneous rocks influenced the deformation of the Permian and Mesozoic sedimentary rocks. In the La Boca–Peregrina structural window, many basement-involved structures on the eastern flank of the Peregrina–Huizachal anticlinorium indicate a westward vergence. Two factors might have contributed to the westward movement. The first comes from folding. The deformation in the limestones is transferred to the underlying less competent strata when the limestones were warped downward. The second factor might be associated with the eastward movement of Precambrian–Paleozoic igneous and metamorphic rocks in the central part of the rift basin. They are generally much more competent than the Permian and Mesozoic sedimentary rocks. Since the Permian and Mesozoic sedimentary rocks are confined by the overlying Jurassic limestone, the eastward movement of the crystalline basement exerts compression from the west and shear traction at the base of the overlying strata, producing a series of west-vergent structures in the overlying Permian and Mesozoic sedimentary rocks. In contrast, no competent basement in the Huizachal structural window exists as that in the La Boca–Peregrina structural window; the deformation in the red beds is strongly influenced by friction along the detachment surface, and resulted in the development of easterly vergent folds. Assuming 60° for the dip of the rift boundary faults, the present hinge zone of the Peregrina anticlinorium moved relative to the projected eastern rift boundary fault approximately 2600 and 1100 m along the Peregrina and Huizachal transects, respectively, indicating a corresponding linear strain of 0.33 and 0.08 for the eastern flank of the anticlinorium.

The basement rise undoubtedly contributed to the deformation of the cover rocks in this area, but its contribution is much less than that in the Rocky Mountains, where deformation of the cover rocks is primarily attributed to forced folding (Stearns, 1978). This is because there are many second- and third-order folds and faults in the cover rocks in the Peregrina–Huizachal anticlinorium. This means that this area is principally dominated by horizontal movement rather than vertical movement. This conclusion agrees with the restored cross-section, indicating that the shortening accommodated by the cover rock is much larger than that in the basement (Fig. 5c).

5. Conclusion

Contractional deformation in the Peregrina–Huizachal anticlinorium is characterized by two phases of deformation: an early thin-skinned phase and a late thick-skinned phase. During the thin-skinned phase a regional detachment developed at the base of Zuloaga Formation. Deformation in the cover rocks is accommodated by flexural slip along bedding, detachment folds and faults. In the Huizachal structural window, asymmetrically tight, overturned folds vergent to the foreland developed in the Mesozoic red beds due to shear traction along the detachment. During the thick-skinned phase, the basement rocks responded to the deformation in various ways for different rocks in the La Boca–Peregrina structural window. For the gneiss, little late stage deformation associated with the development of SMO fold–thrust belt has been observed to overprint pre-existing structures. In contrast, Permian sandstone/shale and Triassic–Jurassic red beds are deformed into a variety of structures vergent to the west. This vergence is ascribed to the down-warping of the overlying limestone and eastward movement of the old hard metamorphic/igneous basement. Uplift of the basement contributed to the formation of Peregrina–Huizachal anticlinorium.

Acknowledgements

Acknowledgment is made to the donors of the American Chemical Society Petroleum Research Fund for support of this research (#39884-G8). Funding for this work is also provided by GSA Research Grant (7566-03). We would like to sincerely thank Professor Timothy Lawton and Thomas G. Blenkinsop for their critical reviews of the manuscript and the helpful suggestions they made. We also thank Paul Burgess for field assistance.

References

Bacon, R.W., 1978. Geology of northern Sierra de Catorce, San Luis Potosi, Mexico. Master Thesis, Arlington, University of Texas, pp. 1–124.

Barboza-Gudino, J.R., Trístan-González, M., Torres-Hernández, J.R., 1999. Tectonic setting of pre-Oxfordian units from central and northeastern Mexico: a review. In: Bartolini, C., Wilson, J.L., Lawton, T.F. (Eds.), Mesozoic Sedimentary and Tectonic History of North-Central Mexico. Geological Society of America Special Paper 340, pp. 197–210.

Basanez-Loyola, M.A., Fernandez-Turner, R., Rosales-Dominguez, C., 1993. Cretaceous platform of Valles-San Luis Potosi, Northeastern Central

Mexico. In: Simo, T., Scott, R.W., Masse, J.P. (Eds.), Cretaceous Carbonate Platforms. American Association of Petroleum Geologists, Memoir 56, pp. 51–59.

Belcher, R.C., 1979. Depositional environments, paleomagnetism, and tectonic significance of Huizachal red beds (Lower Mesozoic), Northeastern Mexico. Master Thesis, University of Texas at Austin.

Butler, R.W.H., Mazzoli, S., Corrado, S., De Donatis, M., Di Bucci, D., Gambini, R., et al., 2004. Applying thick-skinned tectonic models to the Apennine thrust belt of Italy—limitations and implications. In: McClay, K.R. (Ed.), Thrust Tectonics and Hydrocarbon Systems. AAPG Memoir 82, pp. 647–667.

Carrillo-Bravo, J., 1961. Geologia del anticlinoria Peregrina–Huizachal al NW de Ciudad Victoria, Tamaulipas. Asociación Mexicana de Geologos Petroleros Boletin 13, 1–98.

Carrillo-Bravo, J., 1965. Estudio geológico de una parte del Anticlinorio de Huayacocotla. Asociación Mexicana de Geologos Petroleros Boletin 17, 73–96.

Cooper, M.A., Williams, G.D. (Eds.), 1989. Inversion Tectonics. Geological Society (London) Special Publication vol. 44, 375pp.

De Cserna, Z., 1989. An outline of the geology of Mexico. In: Bally, A.W., Palmer, A.R. (Eds.), Decade of North American Geology, Volume A: The Geology of North America—An Overview. Geological Society of America, pp. 233–264.

Dickinson, W.R., Lawton, T.F., 2001. Tectonic setting and sandstone petrofacies of the Bisbee basin. Journal of South American Earth Sciences 14 (5), 475–504.

Eguiluz de Antuñano, S., Aranda-García, M., Marrett, R., 2000. Tectónica de la Sierra Madre Oriental, México. Boletín de la Sociedad Geológica Mexicana 53, 1–26.

Etheridge, M.A., 1986. On the reactivation of extensional fault systems. Royal Society of London Philosophical Transactions A 317, 179–194.

Franco-Rubio, M., 1999. Geology of the basement below the decollement surface, Sierra de Catorce, San Luis Potosi, Mexico. In: Bartolini, C., Wilson, J.L., Lawton, T.F. (Eds.), Mesozoic Sedimentary and Tectonic History of North-Central Mexico. Geological Society of America Special Paper 340, pp. 211–227.

Garrison, J.R., Ramirez-Ramirez, J.C., Long, L.E., 1980. Rb–Sr isotopic study of the ages and provenance of pre-Cambrian granulite and Paleozoic greenschist near Ciudad Victoria, Mexico. In: Pilger, R.H. (Ed.), The Origin of the Gulf of Mexico and the Early Opening of the Central North Atlantic Ocean, pp. 37–50.

Goldhammer, R.K., 1999. Mesozoic sequence stratigraphy and paleogeographic evolution, Northeast Mexico. In: Bartolini, C., Wilson, J.L., Lawton, T.F. (Eds.), Mesozoic Sedimentary and Tectonic History of North-Central Mexico. Geological Society of America Special Paper 340, pp. 1–58.

Holdsworth, R.E., Butler, C.A., Roberts, A.M., 1997. The recognition of reactivation during continental deformation. Geological Society (London) Journal 154, 73–78.

INEGI, 1970. 1:50,000 Estados Unidos Mexicanos geological map.

INEGI, 1977. 1:50,000 Guemez geological map.

INEGI, 1978. 1:50,000 Ciudad Victoria geological map.

INEGI, 2000. 1:250,000 Ciudad Victoria geological map.

Jackson, J.A., Fitch, T.J., Mckenzie, D.P., 1981. Active thrusting and evolution of Zagros fold belt. In: McClay, K.R., Price, N.J. (Eds.), Thrust and Nappe Tectonics. Geological Society, London, Special Publication, vol. 9, pp. 371–380.

Johnson, A.M., 1977. Styles of Folding. Elsevier, New York.

Kley, J., Rossello, T.E., Monaldi, C.R., Habighorst, B., 2005. Seismic and field evidence for selective inversion of Cretaceous normal faults, Salta rift, northwest Argentina. Tectonophysics 399, 155–172.

Lawton, T.F., McMillan, N.J., 1999. Arc abandonment as a cause for passive continental rifting: comparison of the Jurassic Mexican Borderland rift and the Cenozoic Rio Grande rift. Geology 27 (9), 779–782.

Lister, G.S., Snoke, A.W., 1984. S–C mylonites. Journal of Structural Geology 6 (6), 617–638.

López-Ramos, E., 1985. Geologia de Mexico. Tomo II, edición 3a, primera reimpresión, Mexico, D.F. 1985. 453pp.

Marrett, R.A., Aranda, G.M., 1999. Structure and kinematic development of the Sierra Madre Oriental fold belt, Mexico. In: Wilson, J.L., Ward, W.C., Marrett, R. (Eds.), Stratigraphy and Structure of the Jurassic and Cretaceous Platform and Basin Systems of the Sierra Madre Oriental; Monterrey and Saltillo Areas; Northeastern Mexico, a Field Book and Related Papers. South Texas Geological Society, San Antonio, TX, pp. 69–98.

Marshak, S., Karlstrom, K., Timmons, J.M., 2000. Inversion of Proterozoic extensional faults: an explanation for the pattern of Laramide and Ancestral Rockies intracratonic deformation, United States. Geology 28, 735–738.

Mixon, R.B., Murray, G.E., Diaz, G., 1959. Age and correlation of Huizachal Group (Mesozoic), state of Tamaulipas, Mexico. AAPG Bulletin 43, 757–771.

Moran-Zenteno, D., 1994. The geology of the Mexican republic. American Association of Petroleum Geologists Studies in Geology 39, 160.

Padilla y Sanchez, R.J., 1982. Geologic evolution of the Sierra Madre Oriental between Linares, Concepcion del Oro, Saltillo, and Monterrey, Mexico. PhD dissertation, University of Texas at Austin.

Padilla y Sanchez, R.J., 1985. Las estructuras de la Curvature de Monterrey, Estados de Coahuila, Nuevo León, Zacatecas y San Luis Potosi. Instituto de Geologia, Universidad Nacional Autónoma de Mexico, Revista 6, 1–20.

Perez-Cruz, G.A., 1993. Geologic evolution of the Burgos Basin, northeastern Mexico. PhD dissertation, Rice University, 357pp.

Salvador, A., 1987. Late Triassic–Jurassic paleogeography and origin of Gulf of Mexico basin. AAPG Bulletin 71, 419–451.

Sedlock, R.L., Ortega-Gutiérrez, F., Speed, R.C., 1993. Tectonostratigraphic Terranes and Tectonic Evolution of Mexico. Geological Society of America Special Paper 278, 153pp.

Sherkati, S., Molinaro, M., de Lamotte, D.F., Letouzey, J., 2005. Detachment folding in the Central and Eastern Zagros fold-belt (Iran): salt mobility, multiple detachments and late basement control. Journal of Structural Geology 27, 1680–1696.

Sibson, R.H., 1993. Load-strengthening vs. load-weakening faults. Journal of Structural Geology 15, 123–128.

Stearns, D.W., 1978. Faulting and forced folding in the Rocky Mountain fold belt. Geological Society of America Memoir 151, 1–37.

Suter, M., 1987. Structural traverse across the Sierra Madre Oriental fold belt in east-central Mexico. Geological Society of America Bulletin 98, 249–264.

Wilson, J.L., 1990. Basement structural controls on Mesozoic carbonate facies in northeastern Mexico—a review. Special Publications of the International Association of Sedimentologists 9, 235–255.

Wilson, J.L., Ward, W.C., 1993. Early Cretaceous carbonate platforms of northeastern and east-central Mexico. In: Simo, T., Scott, R.W., Masse, J.P. (Eds.), Cretaceous Carbonate Platforms. American Association of Petroleum Geologists Memoir 56, pp. 35–49.